Journal of
Water & Climate Change

Check for updates

IWA PUBLISHING

© 2023 The Authors

Journal of Water and Climate Change Vol 14 No 1, 142 doi: 10.2166/wcc.2022.342

Effect of chemical clogging on the permeability of weakly consolidated sandstone due to reinjection at different temperatures

Tao Zhong[a], Hong Tian[a], Jun Zheng[a], Bin Dou[a,*], Yachao Wang[a], Zhongyan Yang[b], Peng Li[a] and Peng Xiao[a]

[a] Faculty of Engineering, China University of Geosciences (Wuhan), Wuhan 430074, China
[b] Tianjin Geothermal Exploration And Development Designing Institute, Tianjin 300250, China
*Corresponding author. E-mail: doubin@cug.edu.cn

ABSTRACT

While utilizing hydrothermal resources, it is necessary to reinject wastewater into the reservoir through reinjection wells to extract heat without mining groundwater. Chemical clogging is a serious problem in the process of reinjection. The precipitation of minerals can lead to reservoir clogging and the reduction of permeability. Therefore, to study the effect of chemical clogging on permeability, the weakly consolidated sandstone of the Neogene Guantao Formation geothermal reservoir in northern Shandong (Eastern China) was taken as the research object. A long-term thermal-hydro-mechanical-chemistry (THMC) coupling reinjection experiment was carried out. The results showed that when the temperature of wastewater was higher than 45 °C, there was a temporary phase of permeability enhancement in the first 10 min of reinjection. However, wastewater with higher temperatures would cause more chemical clogging eventually. XRD and ion analysis results showed that the precipitation of minerals was mainly potash feldspar, illite, calcite, and other carbonate minerals during reinjection. According to the characteristics of low-TDS wastewater in the Guantao Formation, it is recommended to adopt low-temperature wastewater reinjection and reduce the concentration of Ca^{2+} and Mg^{2+} in wastewater before reinjection.

Key words: chemical clogging, geothermal reinjection, permeability, weakly consolidated sandstone

HIGHLIGHTS

- Water–rock chemical reactions cause the precipitation of minerals.
- Permeability is an important parameter to characterize blockage.
- XRD and ion concentration were used to analyze chemical blockage.
- There was a temporary phase of permeability enhancement in the first 10 min of reinjection.
- Tailwater with higher temperatures will cause more blockage eventually.

This is an Open Access article distributed under the terms of the Creative Commons Attribution Licence (CC BY 4.0), which permits copying, adaptation and redistribution, provided the original work is properly cited (http://creativecommons.org/licenses/by/4.0/).

Downloaded from http://iwaponline.com/jwcc/article-pdf/14/1/142/1165905/jwc0140142.pdf
by guest

GRAPHICAL ABSTRACT

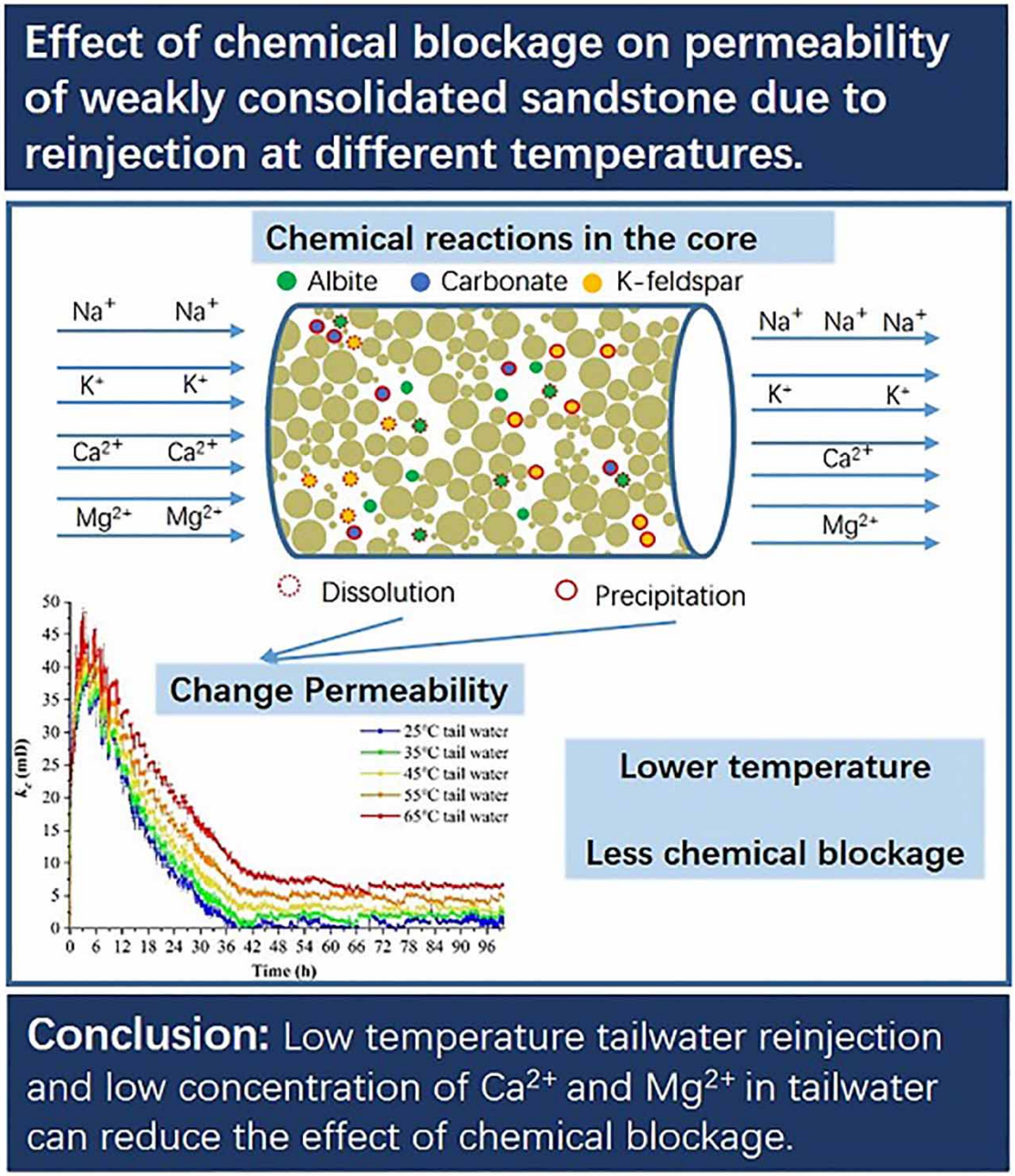

1. INTRODUCTION

With the progress of human civilization and the rapid development of social economy, people are urgently looking for renewable energy to optimize the energy structure. Geothermal energy has attracted more and more attention because of its huge reserves, stable temperature, and low carbon dioxide emissions. China is actively developing and utilizing geothermal resources (Zhao *et al*. 2022). Also, Chinese geothermal resources account for 8% of the whole world (Zhao &Wan 2014).

China is rich in geothermal resources, but only 2.3% of shallow geothermal resources have been exploited (Wang *et al*. 2017). Medium–low temperature hydrothermal geothermal resources are rich in northern Shandong (Wang *et al*. 2015; Kang *et al*. 2021), Kaifeng basin (Lin *et al*. 2007), Qinghai Xining (Zhang *et al*. 2021, 2022a), Guanzhong Basin (Xv *et al*.

Downloaded from http://iwaponline.com/jwcc/article-pdf/14/1/142/1165905/jwc0140142.pdf
by guest

2019), and Tianjin (An *et al*. 2016). Most of them occur in sandstone thermal reservoirs, which are loose porous media. In the process of wastewater reinjection, clogging reduces the permeability, and even causes damage to the reservoir irreversibly (Ungemach 2003; Cui *et al*. 2021a, 2021b, 2022; Zhang *et al*. 2022a, 2022b). Bouwer (2002) proposed that the causes of geothermal reinjection clogging can be mainly divided into suspended solids, microorganisms, bubble clogging, and chemical clogging; Brehme *et al*. (2018) subdivided clogging processes into physical, chemical, and biological processes. Among them, chemical clogging is caused by the change of the original hydrogeochemical equilibrium after wastewater enters the thermal reservoir. To reduce the impact of clogging, it is vital to optimize geothermal reinjection technology (Allow 2013; Diaz *et al*. 2016). At present, all hydrothermal geothermal projects in China require reinjection operations, and the rate of reinjection depends on provincial regulations (Kong *et al*. 2017). However, in actual projects, most geothermal wells cannot achieve continuous reinjection due to clogging. For example, the average reinjection rate of the Neogene Guantao Formation in Tianjin is 34.7%, and 6.3% for the Minghuazhen Formation (Wang 2014). Typical minerals of chemical clogging include carbonates, silicates, sulfates, metal oxides, and clay minerals (Scheiber *et al*. 2012; Haklidir & Haklidir 2017; Ma *et al*. 2017).

The main precipitation in the chemical clogging of geothermal reinjection was the carbonate scale in Xianyang, NW China (Ma *et al*. 2012). Pokrovsky *et al*. (2009) studied the dissolution of calcite and dolomite under different pH, temperature, and CO_2 partial pressure environments rate. The study by Eppner *et al*. (2017) showed that the increase in temperature would reduce the solubility of calcite, which is beneficial to the precipitation of calcite. Moreover, the increase of temperature would also reduce the solubility of CO_2, leading to the precipitation of calcium carbonate. Yang *et al*. (2022a, 2022b) found that the precipitation of carbonate minerals (calcite, dolomite) caused clogging at the back of the column. The concentration of Mg^{2+} can determine the form of carbonate minerals precipitation. Boyd *et al*. (2014) found the higher the Mg^{2+} concentration, the slower the rate of calcite formation, but the faster rate of aragonite formation.

Silicate is prevalent in wastewater and reservoirs, especially in geothermal fields with moderate mineralization and pH (Gallup 1997). Gunnarsson & Arnorsson (2005) stated that the silica scale mainly originates from the monomer amorphous silicas in the process of high-temperature geothermal water recovery and reinjection. Kunan *et al*. (2021) used hydrogeochemical modeling software Phreeqc to reproduce the scaling and the results indicated that silicate precipitation is strongly controlled by kinetic. Potassium feldspar is a kind of silicate. Ngwenya *et al*. (1995) confirmed by SEM, XRD, and ion assay that potassium feldspar can precipitate during reinjection resulting in lower permeability.

Sulfate minerals consist of SO_4^{2-} and cations. The excess of Ca^{2+} and SO_4^{2-} ions can lead to the formation and precipitation of sulfate scales (Cobos *et al*. 2021). Hastie *et al*. (2011) found that the polysulfide can be oxidized to sulfate during the reinjection due to the oxidation of water. Bedrikovetsky *et al*. (2006) combined experimental and mathematical analysis methods to simulate sulfate mineral scaling patterns. Wagner *et al*. (2005) found that gypsum precipitated in warmer regions of the reservoir. Brehme *et al*. (2019) stated that gypsum is more prone to precipitation than barite. Pape *et al*. (2005) investigated the precipitation mechanism of anhydrite. Their results implied that for the same super-saturation anhydrite crystals did not nucleate in small pores, but formed preferentially in large pores.

Metal oxides, especially iron oxides will cause serious clogging if Fe^{2+} is oxidized to Fe^{3+}. Ni *et al*. (2018) found that the presence of both nitrate and oxygen caused Fe^{3+} precipitation. Cobos & Sogaard (2020) stated that reducing iron concentration did not seem to be an efficient method to reduce precipitates if oxygen had not been removed from the fluid. Yin *et al*. (2019) observed that Fe^{2+} was oxidized to Fe^{3+} to generate $Fe(OH)_3$ colloids and adsorbed them in the seepage channels, causing chemical clogging.

Clay minerals are very common in sandstone. Liu *et al*. (2017) stated that the composition of clay minerals is the most important factor that affects the permeability of bine aquifer. They detected that the montmorillonite led to the largest permeability reduction, followed by kaolinite and illite in their further work. Temperature can influence the precipitation of clay minerals. Rosenbrand *et al*. (2014, 2015) discovered heating caused permeability reduction in sandstone formations containing kaolinite clay particles. And a permeability reduction due to heating from 20 to 80 °C was largely reversible with cooling.

Researchers have conducted studies on various aspects of chemical clogging. The reasons for clogging during reinjection depended on the geothermal reservoir and wastewater types. However, nearly all precipitation was affected by temperature, and geothermal wastewater reinjection will form the temperature gradient. Therefore, in this study, we took the weakly consolidated sandstone thermal reservoir of the Guantao Formation in Lubei as an example, simulating the reinjection process at different temperatures. Compared to previous studies, we minimized the impact of physical clogging by setting very low flow velocity. Our study aims to determine the influence of the temperature of wastewater on the chemical clogging in the Lubei

Downloaded from http://iwaponline.com/jwcc/article-pdf/14/1/142/1165905/jwc0140142.pdf
by guest

area. The influence of mineral dissolution and precipitation caused by the change of ion concentration of displacement water on the permeability of the reservoir is emphatically discussed. The results from this study can be used for reducing chemical clogging during wastewater reinjection in the Lubei area.

2. MATERIALS AND METHODS

2.1. Sample characteristics

In the Lubei area, only a small part of bedrock is exposed, and most of them are covered with quaternary sediments, which play a role in the thermal insulation of the lower geothermal reservoir. At present, the main geothermal resource reservoir in this area is the Guantao Formation of Neogene in Cenozoic The lower part of the Guantao Formation is siltstone, conglomerate, and sandy aquitard. The upper part is mainly siltstone, fine sandstone, and medium sandstone, belonging to fluvial facies (Zhang *et al.* 2019; Xv *et al.* 2021).

Guantao Formation sandstone is weakly consolidated fine-grained lithic feldspar sandstone, which is mainly composed of albite, microcline, quartz, Illite/montmorillonite mixed layer, montmorillonite, tremolite, kaolinite, and illite. The particle size ranges from 1.88 to 454 μm and the pore diameter ranges from 20 to 200 μm. The geothermal wastewater is weakly alkaline, and the main ion concentration from high to low is HCO_3^-, Na^+, Cl^-, SO_4^{2-}, CO_3^{2-}, K^+, Ca^{2+}, Mg^{2+}, which is classified as Bicarbonate-sodium water-B type according to the Schukalev classification method (MGMR 1983).

2.1.1. Water sample

To exclude the effects of physical and biological clogging on the results, desanders were used to remove most of the microorganisms, large particles, and suspended particles. The pH of the reinjection water was 8.45, the TDS was 5,237.41 mg/L, and the results of ion analysis are shown in Table 1. The wastewater in the Lubei area has a lower TDS compared with others (Regenspurg *et al.* 2010; Öner *et al.* 2011; Tomaszewska *et al.* 2017; Sasaki *et al.* 2021; Yu *et al.* 2021). A control group of deionized distilled water was also set up to exclude the effects of clogging caused by particle transport, suspended particle transport, water absorption, and swelling of clay.

2.1.2. Rock sample

The rock samples are collected from the Neoproterozoic Guantao Formation in the Lubei geothermal area, and the depth of the samples taken was about 1,100 m, which was in the upper part of the Guantao Formation. Due to the loose cementation, it was difficult to collect, and the complete rock samples obtained were less and small. High-precision rock wire-cutting technology was used to prepare the standard cores required for the reinjection simulation experiments as shown in Figure 1. The

Table 1 | Results of chemical analysis of reinjection water

Ion type	Na^+	K^+	Ca^{2+}	Mg^{2+}	Cl^-	SO_4^{2-}	HCO_3^-	CO_3^{2-}
Mass concentration (mg/L)	470.9	7.66	16.5	2.34	409.3	294.9	3,900.4	135.41

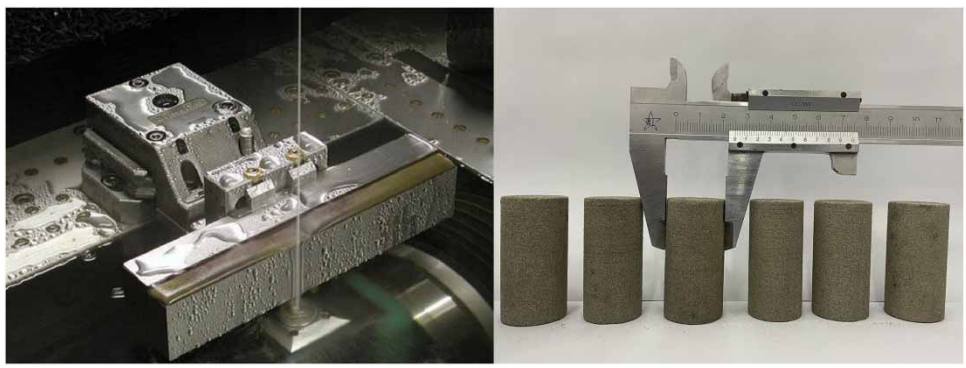

Figure 1 | Rock sample wire-cutting machine and experimental cores.

Downloaded from http://iwaponline.com/jwcc/article-pdf/14/1/142/1165905/jwc0140142.pdf
by guest

median diameter is 0.192 mm initial porosity is 63.821 mD. Rock samples of C1–C6 were prepared for the reinjection experiments. Also, their parameters are shown in Table 2.

2.2. Experimental method

2.2.1. Experimental device

The high temperature and pressure percolation experiment platform is mainly composed of an injection system, model simulation system, metering system, automatic control system, data acquisition, and processing system. The working pressure of the experimental platform can reach up to 60 MPa and the working temperature can reach up to 200 °C. The following steps are required before the experiment begins (Figure 2). In order to exclude the influence of bubble clogging, vacuuming and fulling water should be carried out before the reinjection.

Table 2 | Average of rock sample size and density parameters

Parameters	Unit	C1	C2	C3	C4	C5	C6
Diameter (D)	cm	2.499	2.519	2.509	2.528	2.519	2.520
Length (L)	cm	4.985	4.988	4.990	4.988	4.995	4.989
Area (A)	cm^2	4.906	4.985	4.946	5.025	4.985	4.985
Volume (V)	cm^3	24.458	24.866	24.678	25.063	24.900	24.870
Mass (M)	g	41.91	42.05	43.24	43.63	42.10	42.42
Density (ρ)	g/cm^3	1.714	1.691	1.752	1.741	1.691	1.706

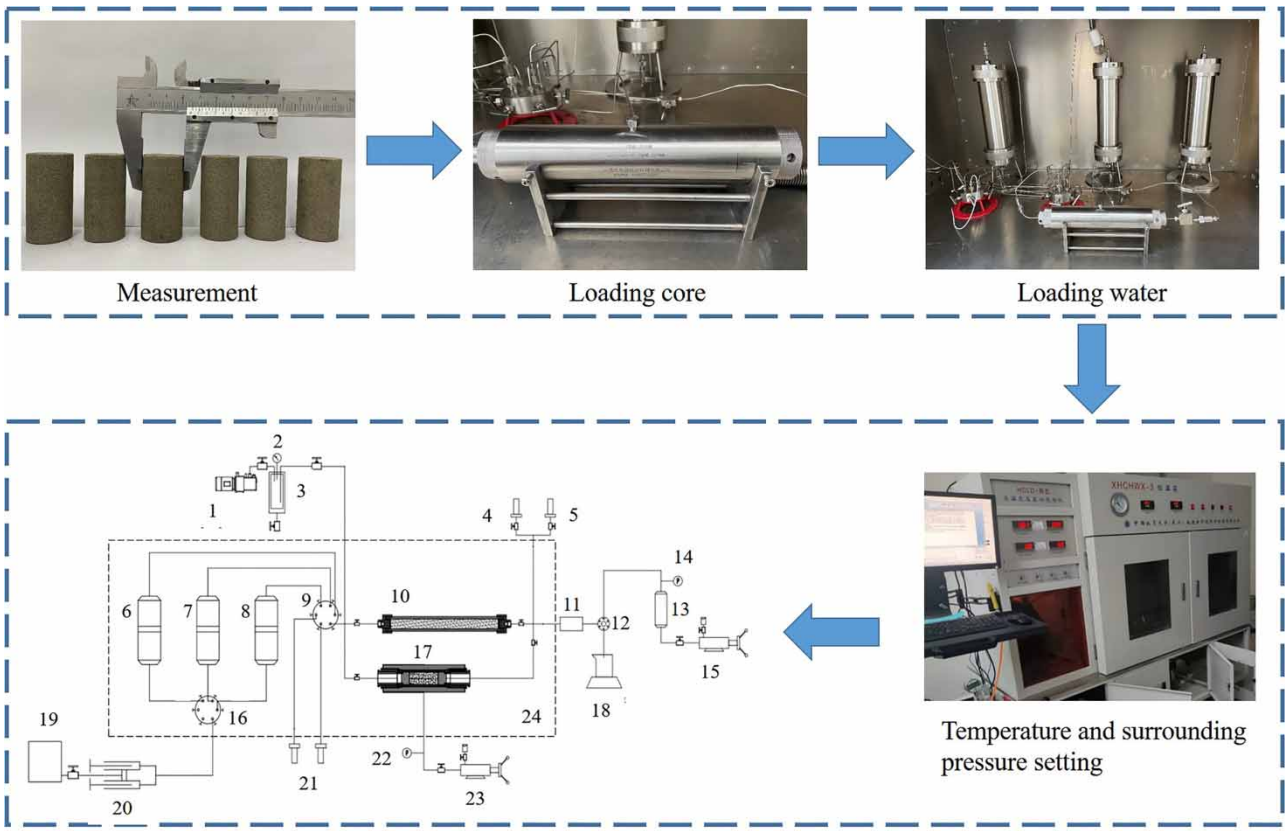

Figure 2 | Test equipment and process diagram. (1) Vacuum pump; (2) Vacuum gauge; (3) Vacuum container; (4) and (5) Pressure sensor (10 MPa); (6)–(8) 1 L container with piston; (9) Six-port valve; (10) Sand-filled pipe; (11) Cooler; (12) Back pressure valve; (13) Back pressure container; (14) Pressure gauge; (15) Hand pump; (16) Six-port valve; (17) Core gripper; (18) Electronic scale; (19) Water Container; (20) Hand pump; (21) Pressure sensor (10 MPa); (22) Pressure gauge; (23) Hand pump; (24) incubator (200 °C).

Downloaded from http://iwaponline.com/jwcc/article-pdf/14/1/142/1165905/jwc0140142.pdf
by guest

2.2.2. Experimental condition

Considering the different temperature gradients caused by low-temperature water and long-term heat extraction, the temperature was set to 25, 35, 45, 55, and 65 °C in this experiment. The depth of the reservoir was about 1,100 m, therefore the surrounding pressure was set to 10 MPa. To fully investigate the effect of water chemistry on clogging during reinjection, and to let the fluid fully contact with the rock sample, the reinjection time was set to 100 h, and the reinjection flow rate was set to 0.5 ml/min (0.0083 cm^3/s). The low flow rate was used to avoid the effect of physical clogging caused by particle migration. The experiments were conducted in constant flow mode, and the pressure values at both ends of the cores were collected in real-time to calculate the permeability. The data were collected every 20 s for each group of experiment, and a total of 120,000 data were collected for 100 h. The experimental conditions were set as shown in Table 3.

2.2.3. Experimental parameters

According to the Core Analysis Method (GB/T 29172-2012), the Darcy expression for the permeability measured by horizontal laminar flow fluid is:

$$k = \frac{\mu q L}{A(P_1 - P_2)} \cdot \frac{1013.25}{600} \tag{1}$$

$$A = \frac{\pi D^2}{4} \tag{2}$$

$$Q = qt \tag{3}$$

where μ is the fluid viscosity, mPa·s; k is the permeability of the medium, mD; q is the volume flow rate, ml/min; A is the cross-sectional area of the core, cm^2; L is the length of the core, cm; D is the diameter of the core, cm; P_1 is the inlet pressure, MPa; P_2 is the outlet pressure, MPa; Q is the reinjection volume, cm^3; t is the reinjection time.

The permeability measured at a certain time may be influenced by various factors, and the chemical clogging permeability measured in this paper is the permeability excluding the effect of particle transport, suspended particle transport, and water absorption and swelling of clay. It is obtained by measuring the permeability of the reinjection displacement group at a certain time minus the permeability of the control group at that time.

$$k_c = k_h - k_d \tag{4}$$

where: k_c is the chemical clogging permeability at a certain moment, mD; k_h is the permeability measured at a certain moment of the wastewater reinjection group, mD; k_d is the permeability measured at a certain moment of the control group, mD.

3. RESULTS

3.1. Evolution of chemical clogging permeability

The change in permeability k of sandstone in each group during the reinjection is shown in Figure 3, and the change of permeability is larger in the 2 h at the beginning of reinjection. The control group was deionized distilled water, which excluded

Table 3 | Experimental condition

Rock sample	Temperature	Flow rate	Surrounding pressure	Displacement time	Fluid type
C1	25 °C	0.5 mL/min	10 MPa	100 h	Deionized distilled water
C2	25 °C				Wastewater
C3	35 °C				Wastewater
C4	45 °C				Wastewater
C5	55 °C				Wastewater
C6	65 °C				Wastewater

Downloaded from http://iwaponline.com/jwcc/article-pdf/14/1/142/1165905/jwc0140142.pdf
by guest

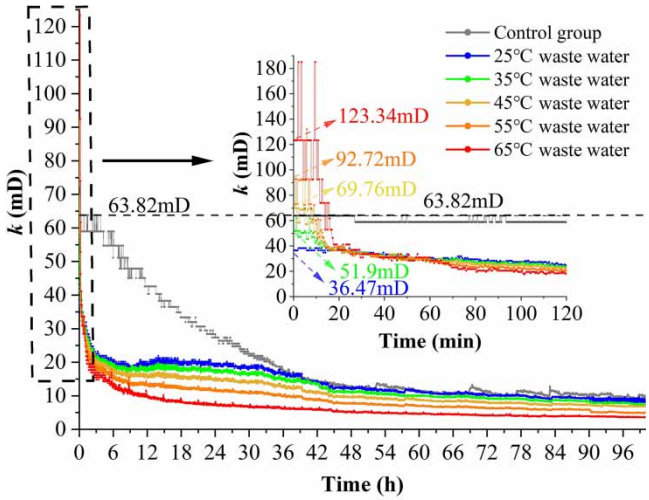

Figure 3 | Permeability k variation in 0–100 h.

the water chemical reaction with bubble clogging and biological clogging that occurred in it. At the beginning of the reinjection, the physical clogging was extremely weak. Therefore, the core permeability of the control group measured at the beginning was chosen to be k_0 of all sandstone samples in this experiment, which is 63.82 mD.

From Figure 3, it can be found that the permeability of each group showed a downward trend over time. The permeability of the control group decreased rapidly in the first two days and then decreased slowly. The permeability of the control group decreased by 7.69, 14.28, 33.33, 80, and 84.46% from 63.82 mD at 1, 6, 12, 48, and 100 h, respectively.

The permeability of the control group did not change within the first 25 min of reinjection displacement. This indicates that the physical clogging and water absorption expansion clogging of the rock sample are very weak when it begins to contact with the wastewater. After 25 min, the physical clogging gradually grew, which indicates that the physical clogging and water absorbing expansion clogging developed gradually through the continuous action of the fluid, and the size of the particles became larger and larger. In the first two days, the pore and throat structure changed and caused the clogging, after that, the pore and throat structure was relatively stable and the permeability was maintained at a low state.

The variation of chemical clogging permeability k_c is obtained by calculation as shown in Figure 4.

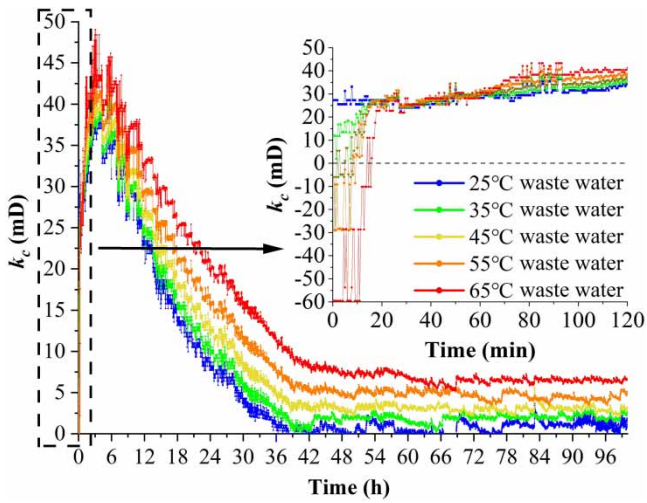

Figure 4 | Permeability k_c variation in 0–100 h.

Downloaded from http://iwaponline.com/jwcc/article-pdf/14/1/142/1165905/jwc0140142.pdf
by guest

On the whole, k_c in all reinjection groups had similar patterns, increasing rapidly in the first 4 h, and the increasing rate gradually decreased. Then k_c started to decline rapidly. The rate of decline gradually decreased, and then it stabilized. In the rapid descent stage, the descent speed first increased and then decreased. The k_c of 25, 35, 45, 55, and 65 °C reinjection groups reached their maximum value at 3.7, 3.9, 4, 4.2, and 4.3 h, respectively. In the first 20 min of reinjection, the higher the temperature of the wastewater, the more drastic the k_c changed. Moreover, in the first 10 min, the k_c of 45, 55 and 65 °C reinjection groups showed negative values, indicating that chemical clogging improved permeability. While the k_c of reinjection groups at 25 and 35 °C was positive, that is, chemical clogging reduced permeability. After 2 days of reaction, k_c of each reinjection temperature group decreased to a relatively stable value. Also, the higher the temperature, the greater the k_c.

3.2. Composition changes during reinjection

The permeability changes of all reinjection groups are generally similar. Taking the reinjection group at 45 °C as an example, XRD test of rock sample C4 was carried out on rock samples before and after reinjection. The changes in mineral composition in rock samples are shown in Table 4. According to the table, after 100 h of wastewater reinjection, the content of albite, tremolite, montmorillonite, and illite/montmorillonite mixed layer in the rock sample decreased. The content of potassium feldspar, illite, and dolomite increased. Kaolinite content did not change. Quartz content increased slightly (Figures 5 and 6).

We collected displacement water of 1, 6, 12, 24, 48, 72, and 100 h at the displacement exit, and analyzed their ion concentration and pH. The results of 45 °C reinjection group after normalization are shown in Figure 7. The original wastewater composition and pH are shown in Table 1. As can be seen from Figure 7, in the reinjection process at 45 °C, the pH of the displacement water decreased in the first 1 h. Then the pH gradually increased, 6 h later slightly higher than the original wastewater wastewater. Then, the pH of the displacement water is lower than that of the original wastewater, showing weak alkalinity. After 48 h, the pH of the displacement water was close to the original wastewater, and the reaction was stable.

Taking the 45 °C reinjection group as an example, it is not difficult to find that if we collected displacement water during the whole reinjection process, only the concentrations of Na^+, Cl^- and SO_4^{2-} will be higher than the original wastewater. Although the concentration of K^+ increased by 26.5% in 1 h. It was lower than original wastewater for the next 80 h. From the aspect of mineral composition, the minerals containing Na^+, Cl^- and SO_4^{2-} were dissolved during the reinjection. XRD results proved that the contents of albite and montmorillonite decreased by 19.64 and 28.61%, respectively, after reinjection, and both of them contained Na^+. Similarly, minerals containing K^+, Ca^{2+}, and Mg^{2+}, such as potash feldspar and

Table 4 | The mineral content changes before and after reinjectioin

Mineral	Albite	Potassium feldspar	Quartz	Tremolite	Montmorillonite	Illite	Kaolinite	Dolomite
Before reinjection	32.49	24.62	24.26	2.47	3.88	0.65	1.78	0
After reinjection	26.11	32.3	24.46	1.96	2.77	0.73	1.78	1.13
Change value	−6.38	7.68	0.2	−0.51	−1.11	0.08	0	1.13
Change degree	−19.64%	31.19%	0.82%	−20.65%	−28.61%	12.31%	0%	–

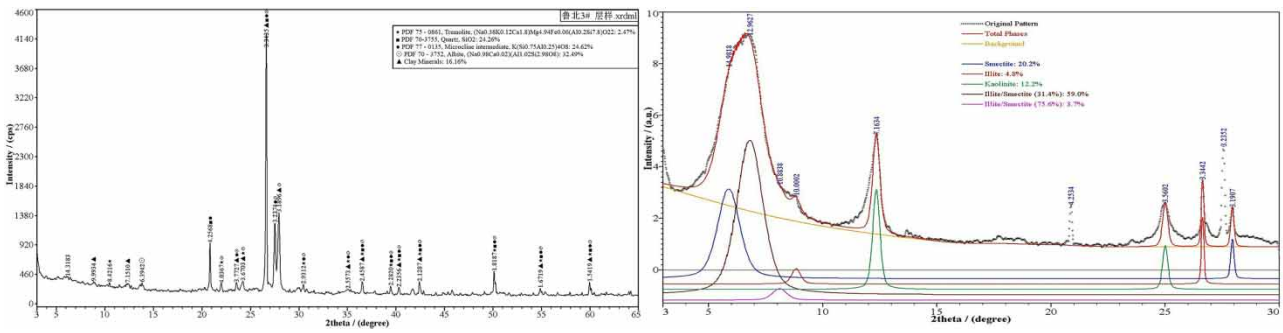

Figure 5 | XRD before reinjection.

Downloaded from http://iwaponline.com/jwcc/article-pdf/14/1/142/1165905/jwc0140142.pdf
by guest

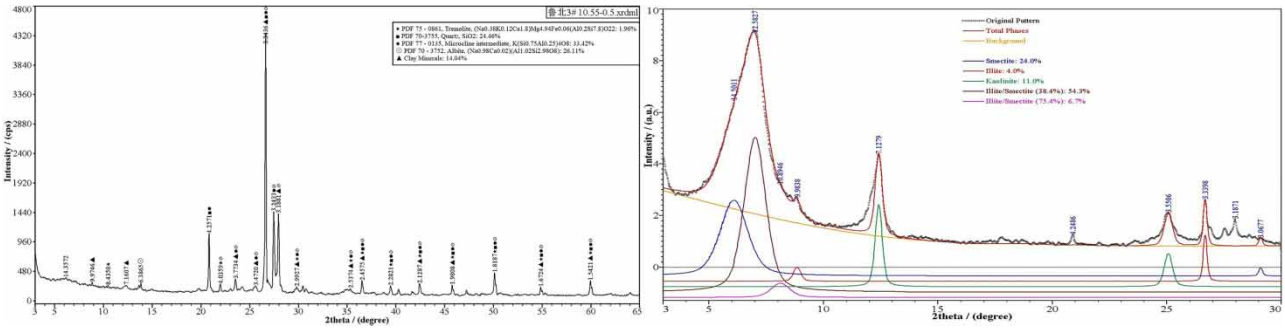

Figure 6 | XRD after reinjection.

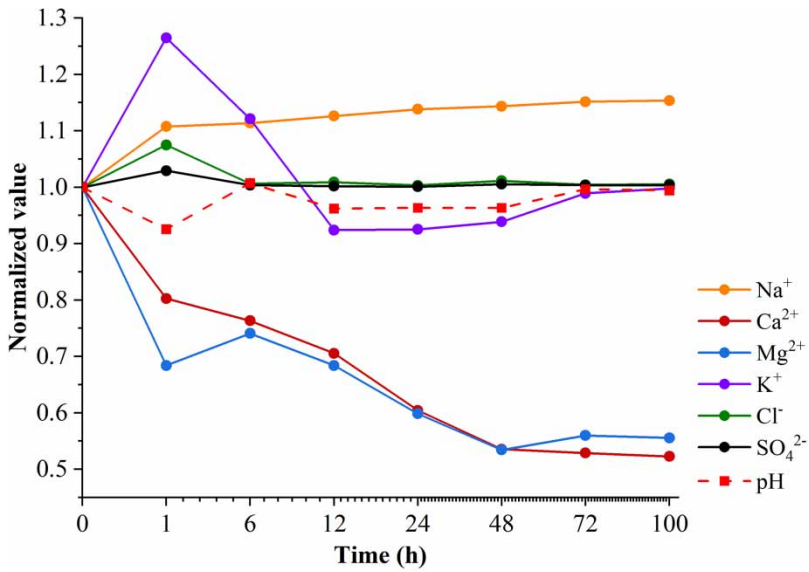

Figure 7 | Normalized ion concentration and pH variation in 0–100 h.

illite, increased by 31.19 and 12.31%, respectively, after reinjection. The calcite was not detected in the original rock samples, but the content increased to 1.13% after reinjection. In general, when the wastewater at different temperatures was reinjected, the reaction inside the rock sample is roughly the same. The increase in temperature will accelerate the rate of chemical reaction, resulting in more precipitation blocking pores.

4. DISCUSSION

4.1. Changes in ion concentration during reinjection

The chemical clogging is due to the change in hydrogeochemical balance after the reinjection water enters the geothermal reservoir (Brehme *et al.* 2018). The composition and structure of water quality and reservoir are changed by water chemical reactions such as dissolution and precipitation. There are many influencing factors of chemical clogging. At present, it is considered that the composition of reinjection water, formation water, mineral composition of geothermal reservoir, temperature, pressure, structure, time, and other factors are the controlling conditions of chemical clogging. (Brehme *et al.* 2019; Song *et al.* 2020; Zhang *et al.* 2021; Gan *et al.* 2022a).

This study recorded the ion concentrations of Na^+, K^+, Ca^{2+}, Mg^{2+}, Cl^-, SO_4^{2-} and the pH at the temperature of 25, 45 and 65 °C (Figure 8). The results indicated that the concentration of Na^+ in the displacement water was higher than in the original wastewater. Increasing temperature can promote the dissolution of minerals containing Na^+. The concentration of K^+

Downloaded from http://iwaponline.com/jwcc/article-pdf/14/1/142/1165905/jwc0140142.pdf
by guest

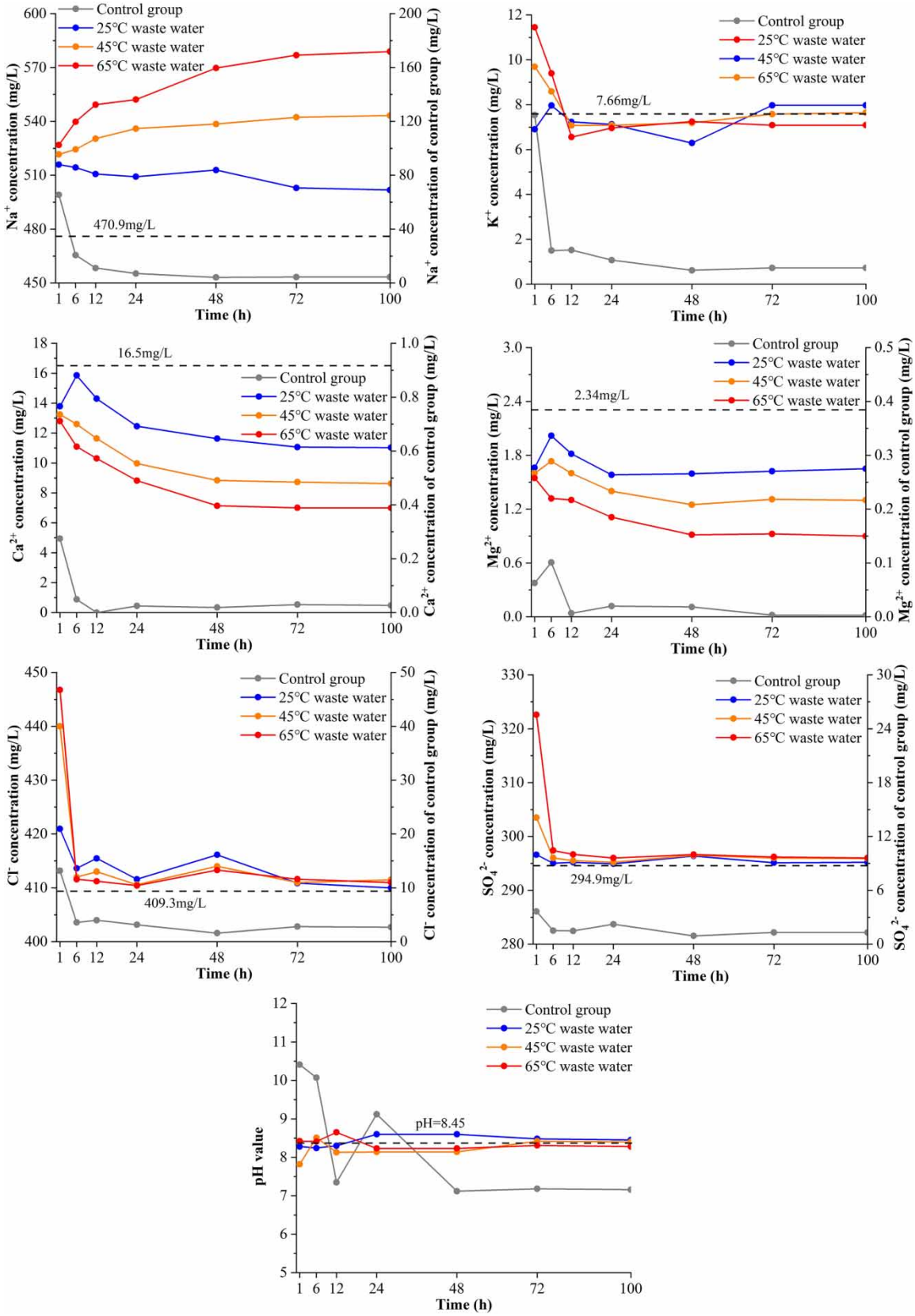

Figure 8 | Ion concentration and pH variation in 0–100 h.

Downloaded from http://iwaponline.com/jwcc/article-pdf/14/1/142/1165905/jwc0140142.pdf
by guest

decreased with the increase of temperature before 6 h, and the concentration of 25 °C reinjection group was lower than that of the original wastewater. Gan *et al.* (2022a; 2022b) observed similar results after 8 h of reinjection. However, they only tested the elements changes before and after the reinjection. We selected seven moments for continuous testing. In our study, the concentration of K^+ in the displacement water increased with the increase in temperature, and the concentration of 65 °C reinjection group was lower than the original wastewater after 72 h. The concentrations of Cl^- and SO_4^{2-} were higher than the original wastewater, and the change was dramatic in the first hour. Both Cl^- and SO_4^{2-} concentrations increased with increasing temperature except Cl^- concentration decreased with increasing temperature from 6 to 48 h. The pH of the displacement water changed frequently in the first 24 h and then became stable. The pH of the 65°C reinjection group was lower than that of the original wastewater, indicating that high temperature promoted the production of H^+.

4.2. Dissolution and precipitation of minerals

The essence of ion concentration change in displacement water was the dissolution and precipitation of minerals. When the albite (NaAlSi3O8) encounters K^+ in the wastewater, it will dissolve and react to form illite, and release Na^+. Yang *et al.* (2022a, 2022b) found the reduction of albite content after 63 days of reinjection was 13.97%. Our XRD results of 45 °C reinjection group showed that the albite decreased by 19.64% and illite increased by 12.31%. As can be seen from the ion concentration in displacement water, the higher the temperature, the faster the reaction. The chemical reactions are provided as following equation:

$$NaAlSi_3O_8 + K^+ + H_2O \leftrightarrow Illite + SiO_2 + OH^- + Na^+ \quad (5)$$

Ngwenya *et al.* (1995) observed that the potash feldspar is dissolved at the displacement inlet and precipitated at the exit. Our results of XRD showed that potassium feldspar increased by 31.19% at 45 °C. Also, the ecreasing of pH in displacement water indicates that the reaction moves toward the formation of potassium feldspar. The chemical reactions are provided as the following equations:

$$KAlSi_3O_8 + H_2O \leftrightarrow Kaolinite + SiO_2 + OH^- + K^+ \quad (6)$$

$$KAlSi_3O_8 + H^+ \leftrightarrow Illite + SiO_2 + K^+ + H_2O \quad (7)$$

Montmorillonite ($(Na,Ca)_{0.33}(Al,Mg)_2[Si_4O_{10}](OH)_2{\cdot}nH_2O$) contains K^+, Na^+, Ca^{2+}, and Mg^{2+}. It will promote the formation of carbonate precipitation and sulfate precipitation during the dissolution process. The XRD of 45-°C reinjection group showed that montmorillonite decreased by 28.61% and calcite was not detected before reinjection, but 1.13% after reinjection. wastewater contains large amounts of CO_3^{2-} and SO_4^{2-}, which can promote the dissolution of tremolite to form carbonate and sulfate precipitation The XRD of 45°C reinjection group showed that the tremolite decreased by 20.65%. The chemical reactions are provided as Equations (8)–(11):

$$Ca^{2+} + CO_3^{2-} \leftrightarrow CaCO_3 \downarrow \quad (8)$$

$$Mg^{2+} + CO_3^{2-} \leftrightarrow MgCO_3 \downarrow \quad (9)$$

$$Mg^{2+} + SO_4^{2-} \leftrightarrow MgSO_4 \downarrow \quad (10)$$

$$Ca^{2+} + SO_4^{2-} \leftrightarrow CaSO_4 \downarrow \quad (11)$$

The precipitation of minerals is affected by the temperature, especially the carbonate precipitation. Its solubility decreases with increasing temperature (Pokrovsky *et al.* 2009; Ma *et al.* 2017). On the contrary, the solubility of sulfate minerals such as gypsum ($CaSO_4$) increases with increasing temperature (Pape *et al.* 2005).

To reduce the impact of chemical clogging, low-temperature wastewater should be used for reinjection (He *et al.* 2018; Kamila *et al.* 2021; Gan *et al.* 2022a). High-temperature wastewater can only dissolve some minerals in the reservoir at the beginning, temporarily improving the permeability of the reservoir. In the end, due to higher temperature, the chemical reaction in the reservoir is accelerated, which will reduce the reservoir permeability more. In addition, Ca^{2+} and Mg^{2+} can be removed before reinjection, which can avoid the decline of permeability caused by the production of potash feldspar, illite, and calcite.

Downloaded from http://iwaponline.com/jwcc/article-pdf/14/1/142/1165905/jwc0140142.pdf
by guest

5. CONCLUSIONS

In this paper, the permeability evolution of weakly consolidated sandstone in the process of wastewater reinjection at different temperatures was analyzed through reinjection and hydrochemical experiments. The main conclusions are as follows:

- The permeability of the rock samples was 63.821 mD, and the permeability decreased due to chemical clogging at the end of reinjection. It decreased faster in the first 2 days. After 100 h of reinjection, the permeability of rock samples C1–C6 decreased to 15.39, 13.64, 11.68, 10.71, 7.87 and 5.68%, respectively.
- In this paper, we used the permeability of wastewater reinjection group minus the permeability of the control group at a certain moment as chemical clogging permeability k_c to express the degree of chemical clogging during reinjection. If the wastewater temperature reached 45 °C or higher, the chemical clogging permeability will be negative in the first 10 min, so that the reservoir permeability can be temporarily improved. After that, the chemical clogging permeability became positive, and the higher the temperature, the more clogging will eventually be caused.
- Compared with the original wastewater, the concentration of Na^+, Cl^- and SO_4^{2-} in the displacement water increased, while the concentration of K^+, Ca^{2+}, and Mg^{2+} decreased finally. It is suggested that the chemical clogging of reinjection is mainly caused by potash feldspar and illite, calcite, and other carbonate precipitation. As the temperature increased, the chemical clogging in rock samples became worse. To reduce the influence of chemical clogging, it is recommended to adopt low-temperature reinjection for the low TDS of wastewater in the Lubei area, and reducing the concentration of Ca^{2+} and Mg^{2+} in wastewater before reinjection is also beneficial for reducing chemical clogging.

FUNDING

This research work was supported by National Key R&D Program of China (Grant Number 2019YFB1504201).

DATA AVAILABILITY STATEMENT

All relevant data are included in the paper or its Supplementary Information.

CONFLICT OF INTEREST

The authors declare there is no conflict.

REFERENCES

Allow, K. 2013 Hypothetical thermohaline transportation study of pumping-reinjection wells in the geothermal field. *Arabian Journal of Geosciences* **6** (2), 409–417.

An, Q., Wang, Y., Zhao, J., Luo, C. & Wang, Y. 2016 Direct utilization status and power generation potential of low-medium temperature hydrothermal geothermal resources in Tianjin, China: a review. *Geothermics* **64**, 426–438.

Bedrikovetsky, P., Mackay, E., Moraes, G., Rosario, F. & Monteiro, R. 2006 Laboratory-based prediction of sulphate scaling damage. In *SPE International Oilfield Scale Symposium*, Aberdeen, United Kingdom.

Bouwer, H. 2002 Artificial recharge of groundwater: hydrogeology and engineering. *Hydrogeology Journal* **10** (1), 121–142.

Boyd, V., Yoon, H., Zhang, C., Oostorm, M., Hess, N., Fouke, B., Valocchi, A. & Werth, C. 2014 Influence of Mg^{2+} on $CaCO_3$ precipitation during subsurface reactive transport in a homogeneous silicon-etched pore network. *Geochimica et Cosmochimica Acta* **135**, 321–335.

Brehme, M., Regenspurg, S., Leary, P., Bulut, F., Milsch, H., Petrauskas, S., Valickas, R. & Blöcher, G. 2018 Injection-triggered occlusion of flow pathways in geothermal operations. *Geofluids* **2018**, 4694829.

Brehme, M., Nowak, K., Banks, D., Petrauskas, S., Valickas, R., Bauer, K., Burnside, N. & Boyce, A. 2019 A review of the hydrochemistry of a deep sedimentary aquifer and its consequences for geothermal operation: Klaipeda, Lithuania. *Geofluids* **2019**, 4363592.

Cobos, J. & Sogaard, E. 2020 Study of geothermal brine reinjection by microcalorimetry and core flooding experiments. *Geothermics* **87**, 101863.

Cobos, J., Knudby, C. & Sogaard, E. 2021 A geothermal plant from a time-scale perspective. *Energies* **14** (19), 6069.

Cui, G., Pei, S., Rui, Z., Dou, B., Ning, F. & Wang, J. 2021a Whole process analysis of geothermal exploitation and power generation from a depleted high-temperature gas reservoir by recycling CO_2. *Energy* **217**, 119340.

Cui, G., Ren, S., Dou, B. & Ning, F. 2021b Geothermal energy exploitation from depleted high-temperature gas reservoirs by recycling CO_2: the superiority and existing problems. *Geoscience Frontiers* **12** (6), 101078.

Cui, G., Ning, F., Dou, B., Tong, L. & Zhou, Q. 2022 Particle migration and formation damage during geothermal exploitation from weakly consolidated sandstone reservoirs via water and CO_2 recycling. *Energy* **240**, 122507.

Downloaded from http://iwaponline.com/jwcc/article-pdf/14/1/142/1165905/jwc0140142.pdf
by guest

Diaz, A., Kaya, E. & Zarrouk, S. 2016 Reinjection in geothermal fields A worldwide review update. *Renewable & Sustainable Energy Reviews* **53**, 105–162.

Eppner, F., Pasquier, P. & Baudron, P. 2017 A coupled thermo-hydro-geochemical model for standing column well subject to CO_2 degassing and installed in fractured calcareous aquifers. *Geomechanics for Energy and The Environment* **11**, 14–27.

Gallup, D. 1997 Aluminum silicate scale formation and inhibition: scale characterization and laboratory experiments. *Geothermics* **26** (4), 483–499.

Gan, H., Liu, Z., Wang, G., Liao, Y., Xiao Wang, X., Zhang, Y., Zhao, J. & Liu, Z. 2022a Permeability and porosity changes in sandstone reservoir by geothermal fluid reinjection: insights from a laboratory study. *Water* **14** (19), 3131.

Gan, H., Liu, Z., Wang, X., Liao, Y., Xiao Wang, X., Zhang, Y., Zhao, G., Zhao, J. & Liu, Z. 2022b Effect of temperature and acidification on reinjection of geothermal water into sandstone geothermal reservoirs: laboratory study. *Water* **14** (19), 2955.

Gunnarsson, I. & Arnorsson, S. 2005 Impact of silica scaling on the efficiency of heat extraction from high-temperature geothermal fluids. *Geothermics* **34** (3), 320–329.

Haklidir, F. & Haklidir, M. 2017 Fuzzy control of calcium carbonate and silica scales in geothermal systems. *Geothermics* **70**, 230–238.

Hastie, J., Bejan, D. & Bunce, N. 2011 Oxidation of sulfide ion in synthetic geothermal brines at carbon-based anodes. *Canadian Journal of Chemical Engineering* **89** (4), 948–957.

He, M., Zhang, L., Yuan, Y., Zhang, J. & Gao, Y. 2018 Study on the relationship between re-injection volume and temperature of sandstone geothermal reservoir in Nanzhan area of Dongying City. *Shandong Land Resources* **34**, 44–48.

Kamila, Z., Kaya, E. & Zarrouk, S. J. 2021 Reinjection in geothermal fields: an updated worldwide review. *Geothermics* **89**, 101970.

Kang, F., Yang, X., Wang, X. & Zheng, T. 2021 Hydrothermal features of a sandstone geothermal reservoir in the north Shandong plain, China. *Lithosphere* **2021**, 1675798.

Kong, Y., Pang, Z., Shao, H. & Kolditz, O. 2017 Optimization of well-doublet placement in geothermal reservoirs using numerical simulation and economic analysis. *Environmental Earth Sciences* **76**, 118.

Kunan, P., Ravier, G., Dalmais, E. & Cezac, P. 2021 Thermodynamic and kinetic modelling of scales formation at the Soultz-sous-Forets geothermal power plant. *Geosciences* **11** (12), 483.

Lin, X., Taboure, A., Wang, X. & Liao, Z. 2007 Use of a hydrogeochemical approach in determining hydraulic connection between porous heat reservoirs in Kaifeng area, Henan, China. *Applied Geochemistry* **22** (2), 276–288.

Liu, X., Jiang, X., Liu, J., Li, J. & Li, W. 2017 The effect of the injection salinity and clay composition on aquifer permeability. *Applied Thermal Engineering* **118**, 551–560.

Ma, Z., Yan, H., Zhou, X. & Hou, C. 2012 Impact of carbonate scaling on the efficiency of used geothermal water reinjection from low-middle temperature geothermal fluid in xianyang porous geothermal field, NW China. *Advanced Materials Research* **614–615**, 307–310.

Ma, Z., Xu, Y., Zhai, M. & Wu, M. 2017 Clogging mechanism in the process of reinjection of used geothermal water: a simulation research on Xianyang No.2 reinjection well in a super-deep and porous geothermal reservoir. *Journal of Groundwater Science and Engineering* **5** (4), 311–325.

MGMR 1983 *Hydrogeological Manual, Hydrogeological Engineering and Geological Technique Research Team, Ministry of Geology and Mineral Resources, The People's Republic of China*. Geology Publishing House, Beijing, pp. 105–108.

Ngwenya, B., Elphick, S. & Shimmield, G. 1995 Reservoir sensitivity to water flooding – an experimental-study of seawater injection in a north-sea reservoir analog. *AAPG Bulletin-American Association of Petroleum Geologists* **79** (2), 285–304.

Ni, Z., Gaans, P., Rijnaarts, H. & Grotenhuis, T. 2018 Combination of aquifer thermal energy storage and enhanced bioremediation: biological and chemical clogging. *Science of The Total Environment* **613**, 707–713.

Öner, Ş. G., Kabay, N., Güler, E., Kitişb, M. & Yüksela, M. 2011 A comparative study for the removal of boron and silica from geothermal water by cross-flow flat sheet reverse osmosis method. *Desalination* **283**, 10–15.

Pape, H., Clauser, C., Iffland, J., Krug, R. & Wagner, R. 2005 Anhydrite cementation and compaction in geothermal reservoirs: interaction of pore-space structure with flow, transport, P-T conditions, and chemical reactions. *International Journal of Rock Mechanics and Mining Sciences* **42** (7–8), 1056–1069.

Pokrovsky, O., Golubev, S., Schott, J. & Castillo, A. 2009 Calcite, dolomite and magnesite dissolution kinetics in aqueous solutions at acid to circumneutral pH, 25 to 150 degrees C and 1 to 55 atm pCO_2: new constraints on CO_2 sequestration in sedimentary basins. *Chemical Geology* **265** (1–2), 20–32.

Regenspurg, S., Wiersberg, T., Brandt, W., Huenges, E., Saadat, A., Schmidt, K. & Zimmerman, G. 2010 Geochemical properties of saline geothermal fluids from the in-situ geothermal laboratory Gross Schonebeck (Germany). *Chemie Der Erde-Geochemistry* **703**, 3–12.

Rosenbrand, E., Haugwitz, C., Jacobsen, P., Kjoller, C. & Fabricius, I. 2014 The effect of hot water injection on sandstone permeability. *Geothermics* **50**, 155–166.

Rosenbrand, E., Kjoller, C., Riis, J., Kets, F. & Fabricius, I. 2015 Different effects of temperature and salinity on permeability reduction by fines migration in Berea sandstone. *Geothermics* **53**, 225–235.

Sasaki, K., Morita, J., Iwaki, C. & Ueda, A. 2021 Geochemical evaluation of geothermal resources in Toyama Prefecture, Japan, based on the chemical and isotopic characteristics of hot spring waters. *Geothermics* **93**, 102071.

Scheiber, J., Nitschke, F., Seibt, A. & Genter, A. 2012 *Geochemical and Mineralogical Monitoring of the Geothermal Power Plant in Soultz-Sous-Forêts (France)*.

Song, W., Liu, X., Zheng, T. & Yang, J. 2020 A review of recharge and clogging in sandstone aquifer. *Geothermics* **87**, 101857.

Downloaded from http://iwaponline.com/jwcc/article-pdf/14/1/142/1165905/jwc0140142.pdf
by guest

Tomaszewska, B., Rajca, M., Kmiecik, E., Bodzek, M., Bujakowski, W., Wątor, K. & Tyszer, M. 2017 The influence of selected factors on the effectiveness of pre-treatment of geothermal water during the nanofiltration process. *Desalination* **406**, 74–82.

Ungemach, P. 2003 Reinjection of cooled geothermal brines into sandstone reservoirs. *Geothermics* **32** (4), 743–761.

Wagner, R., Kuhn, M., Meyn, V., Pape, H., Vath, U. & Clauser, C. 2005 Numerical simulation of pore space clogging in geothermal reservoirs by precipitation of anhydrite. *International Journal of Rock Mechanics and Mining Sciences* **42** (7–8), 1070–1081.

Wang, L. 2014 *A Study of Geothermal Reinjection in the Guantao Reservoir in Tianjian*. China University of Geosciences, Beijing.

Wang, J., Jin, M., Jia, B. & Kang, F. 2015 Hydrochemical characteristics and geothermometry applications of thermal groundwater in northern Jinan, Shandong, China. *Geothermics* **57**, 185–195.

Wang, G., Zhang, W., Liang, J., Lin, W., Liu, Z. & Wang, W. 2017 Evaluation of geothermal resources potential in China. *Acta Geoscientica Sinica* **38**, 449–459.

Xv, P., Li, M., Qian, H., Zhang, Q., Liu, F. & Hou, K. 2019 Hydrochemistry and geothermometry of geothermal water in the central Guanzhong Basin, China: a case study in xi'an. *Environmental Earth Sciences* **78** (3), 87.

Xv, T., Zhao, Y., Zhao, J., Zhang, L., Liu, S., Liu, Z., Feng, B., Feng, G. & Yue, G. 2021 Heat extraction performance and optimization for a doublet-well geothermal system in Dezhou, China. *Energy Exploration & Exploitation* **40** (2), 619–638.

Yang, J., Ren, W., Kang, B. & Tao, Y. 2022a Experimental investigation on chemical clogging mechanism of loose porous media in recharge process of groundwater heat pump. *Environmental Technology* **12**, 1–17.

Yang, J., Tao, Y., Gao, Y., Wang, L. & Kang, B. 2022b Experimental study on the water–rock interaction mechanism in a groundwater heat pump reinjection process. *Journal of Water & Climate Change* **13** (3), 1516.

Yin, S., Shao, Y., Wu, A., Wang, S. & Li, G. 2019 The effect of ferrous ions on hydraulic conductivity in fine tailings. *Engineering Geology* **260**, 105243.

Yu, X., Liu, C., Wang, C., Zhao, J. & Wang, J. 2021 Origin of geothermal waters from the upper cretaceous to lower eocene strata of the Jiangling Basin, South China: constraints by multi-isotopic tracers and water-rock interactions. *Applied Geochemistry* **124**, 104810.

Zhang, W., Wang, G., Liu, F., Xing, L. & Li, M. 2019 Characteristics of geothermal resources in sedimentary basins. *Geology in China* **46** (02), 255–268.

Zhang, L., Geng, S., Yang, L., Wen, R., He, C., Zhao, Z. & Qin, G. 2021 Formation blockage risk analysis of geothermal water reinjection: rock property analysis, pumping and reinjection tests, and long-term reinjection prediction. *Geoscience Frontiers* **13**, 101299.

Zhang, L., Geng, S., Chao, J., Yang, L., Zhao, Z., Qin, G. & Ren, S. 2022a Scaling and blockage risk in geothermal reinjection wellbore: experiment assessment and model prediction based on scaling deposition kinetics. *Journal of Petroleum Science and Engineering* **209**, 109867.

Zhang, L., Yang, L., Geng, S., Wen, R., He, C. & Liang, Y. 2022b Numerical simulation study on the heat extraction capacity of self-circulation wellbore and its enhanced methods in porous medium-low temperature geothermal reservoirs. *Renewable Energy* **194**, 1009–1025.

Zhao, X. & Wan, G. 2014 Current situation and prospect of China's geothermal resources. *Renewable & Sustainable Energy Reviews* **32**, 651–661.

Zhao, X., Ma, X., Chen, B., Shang, Y. & Song, M. 2022 Challenges toward carbon neutrality in China: strategies and countermeasures. *Resources Conservation and Recycling* **176**, 105959.

First received 27 June 2022; accepted in revised form 4 December 2022. Available online 22 December 2022

Downloaded from http://iwaponline.com/jwcc/article-pdf/14/1/142/1165905/jwc0140142.pdf
by guest